

NJC

Accepted Manuscript



This is an *Accepted Manuscript*, which has been through the Royal Society of Chemistry peer review process and has been accepted for publication.

Accepted Manuscripts are published online shortly after acceptance, before technical editing, formatting and proof reading. Using this free service, authors can make their results available to the community, in citable form, before we publish the edited article. We will replace this *Accepted Manuscript* with the edited and formatted *Advance Article* as soon as it is available.

You can find more information about *Accepted Manuscripts* in the [Information for Authors](#).

Please note that technical editing may introduce minor changes to the text and/or graphics, which may alter content. The journal's standard [Terms & Conditions](#) and the [Ethical guidelines](#) still apply. In no event shall the Royal Society of Chemistry be held responsible for any errors or omissions in this *Accepted Manuscript* or any consequences arising from the use of any information it contains.

Efficient sorption of Pb(II) from aqueous solution using poly (aniline-co-3-aminobenzoic acid) - based magnetic core-shell nanocomposite

Ehsan Nazarzadeh Zare*, Moslem Mansour Lakouraj, Atefeh Ramezani

Polymer research laboratory, Department of Organic-Polymer Chemistry, Faculty of Chemistry, University of Mazandaran, Babolsar, Iran

*Corresponding author Email: ehsan.nazarzadehzare@gmail.com; Tel-fax: +981125342350;

Postal code: 47416-95447

Abstract

Novel poly (aniline-co-3-aminobenzoic acid)-based magnetic core-shell (PA3ABA@Fe₃O₄) nanocomposite was successfully synthesized via an in-situ copolymerization approach of aniline and 3-aminobenzoic acid in the presence of Fe₃O₄ magnetic nanoparticles. The products were characterized by Fourier transformed infrared (FT-IR), proton nuclear magnetic resonance (¹H-NMR), X-ray diffraction (XRD), thermo gravimetric analysis (TGA) and scanning electron microscopy (SEM). Transmission electron microscopy (TEM) image of the PA3ABA@Fe₃O₄ nanocomposite was showed a core-shell structure. Magnetic measurement displayed that the PA3ABA@Fe₃O₄ nanocomposite was super-paramagnetic with saturation magnetization (M_s), 37.8 emu/g. Then, uptake of Pb(II) from aqueous solution by products was investigated as a function of as a function of pH, adsorption dosage, contact time, and initial concentration of Pb(II) through batch studies. The PA3ABA@Fe₃O₄ nanocomposite exhibited higher adsorption percentage (89%) than that of the PA3ABA (80%) for uptake of Pb(II). The PA3ABA@Fe₃O₄ nanocomposite adsorbent could be easily separated from aqueous solution by a magnet and regenerated easily by acid treatment. The experimental data were analyzed by isotherm and kinetic models. The results showed that the interaction between Pb(II) and PA3ABA@Fe₃O₄ nanocomposite in agreement with the Freundlich isotherm and pseudo-first-order kinetic model and the maximum adsorption capacity (Q_m) of Pb(II) was found 138.31 (mg g⁻¹). Therefore, PA3ABA@Fe₃O₄ nanocomposite could be considered as a promising adsorbent for Pb(II) removal from water.

Keywords: Removal of Pb(II), poly (aniline-co-3-aminobenzoic acid), magnetic core-shell nanocomposite, isotherm, kinetic

Introduction

Heavy metals pollution including Cr(VI), Cu (II), Zn(II), Ni(II), and Pb(II) ions have developed a serious universal problem that endangers the environment and health of human beings.¹ So, the effective elimination and recovery of industrial heavy metal ions from wastewater are important interest both an environmental viewpoint and a resource viewpoint. Among these heavy metal ions, Pb(II) is known for its high priority toxic and can cause various symptoms, such as central nervous system damage, liver disease, lung cancer, kidney damage, vomiting, and severe diarrhea.² Pb(II), can reach the environment from natural geochemical processes as well as from various process industries, such as acid metal plating and finishing, battery manufacturing, and ceramic and glass industries.³ Thus, the elimination of Pb(II) from wastewater seems to be a significant and vital task.

Till now, many conventional treatment techniques are used to remove heavy metal ions from water include reverse osmosis, chemical precipitation, nanofiltration, electro ion exchange, coagulation, and adsorption.² Among these techniques, adsorption is the most promising technique due to, its simplicity, fitness, and high removal efficiency that make it a potentially cost-effective method for the elimination of toxic heavy metals from wastewater.⁴

Conductive polymers (CPs) such as polypyrrole (PPy), polyaniline (PAni), and polythiophene (PTh) have attracted the most attention, due to their unique properties, such as ease of synthesis, high stability under ambient conditions, and variable conductivity.⁵⁻⁷ In specific, CPs contain of heteroatom, e.g., N atom in PAni and PPy, and S atom in PTh, play a significant role in toxic metal ions elimination from aqueous solutions by chelation.^{7, 8-16}

On the other hand, easy operation is also a very essential property for the ideal adsorbent. Magnetic separation, in comparison with other techniques such as precipitation, centrifugation,

and filtration, has revealed facile operation and reduced capital costs.¹⁷ Consequently, the composite systems with magnetic nanoparticles have been extensively used in the adsorption process to improve separation after water treatment. Different types of adsorbents have been reported for the removal of pollutants from water.^{4, 17-25}

To the best of our knowledge, there is no study on the poly (aniline-co-3-aminobenzoic acid)@Fe₃O₄ (PA3ABA@Fe₃O₄) core-shell nanocomposite as an adsorbent for the removal of Pb(II) from aqueous solution has not been reported before. The objective of this research was synthesis of PA3ABA@Fe₃O₄ core-shell nanocomposite as an adsorbent for the removal of Pb(II) by a two-step method through the co-precipitation technique and in-situ chemical radical copolymerization. The products were characterized by Fourier transform infrared (FTIR), proton nuclear magnetic resonance (¹H-NMR), X-ray diffraction (XRD), scanning electron microscopy (SEM), transmission electron microscopy (TEM), thermal gravimetric analysis (TGA), and vibrating sample magnetometer (VSM), respectively. The adsorption behavior onto the synthesized materials was studied under different conditions, including various contact times, pH, adsorbent dosages, and initial concentrations. Adsorption kinetic and isotherm models of the synthesized adsorbents were investigated by famous equations to determine the adsorption kinetic and isotherm parameters.

Materials

Aniline (Ani) (Merck-Germany) was purified by double distillation under the reduced pressure and stored in a refrigerator before use. Ammonium persulfate (APS), 3-aminobenzoic acid (3ABA), ammonium hydroxide, FeCl₃·6H₂O, FeCl₂·4H₂O and the used solvents were

purchased from Merck company, Germany. Standard solution of Pb(II) was prepared from $\text{Pb}(\text{NO}_3)_2$ salt (1000 mg L^{-1}) standard solution.

Instruments

FTIR analysis was carried out on a Bruker Tensor 27 spectrometer (Bruker, Karlsruhe, Germany). Samples were prepared by dispersing in dry KBr pellets and recorded between 4000 and 400 cm^{-1} . ^1H NMR spectrum was recorded on a 400 MHz Bruker Avance DRX spectrometer (Germany) in DMSO-d_6 using tetramethyl silane as an internal reference. The surface morphology of the materials was examined by using scanning electron microscopy (SEM) (Model: Hitachi S4160, Japan). Transmission electron microscopy (TEM) was performed on a CM1 electron microscope at an accelerating voltage of 120 kV (Philips, Netherland). The X-ray diffraction (XRD, Shibuya-ku, Japan) patterns were recorded at room temperature on a RigakuD/Max-2550 powder diffractometer with a scanning rate of 5° min^{-1} , and recorded in the 2θ range of $10\text{--}70^\circ$. Thermo-gravimetric analysis (TGA) of prepared adsorbents was investigated using the LENSES STAPT-1000 calorimeter (Germany) by scanning up to 800°C with the heating rate of $10^\circ\text{C}/\text{min}$. A PHS-3C pH-meter (Shanghai, Tianyou) was used for pH measurements. The Pb(II) concentration in the solution was measured by use of a flame atomic absorption spectrophotometer (AAS) (Hewlett-Packard 3510, Germany). VSM measurement was performed by using a vibrating sample magnetometer (Daghigh Kavir Co, Kashan, Iran). The magnetization measurements were carried out in an external field up to 15 kOe at room temperature. Sonication agitation was carried out on a Soner 220H Ultrasonic Cleaner, AC110V, 60 Hz (Taiwan).

Preparation procedures

Synthesis of poly (aniline-co-3-aminobenzoic acid) copolymer

Poly (aniline-co-3-aminobenzoic acid) (PA3ABA) copolymer was prepared of Ani and 3ABA by chemical oxidative copolymerization according to our previous work.²⁶ Typically, 1 g (0.010 mol) of Ani monomer and 1.46 g (0.010 mol) of 3ABA were added to 50 mL of HCl solution (1 M) and then solution was dispersed under magnetic stirring for 30 min and ultrasonication for 40 min to obtain a uniform mixture. Copolymerization was initiated by the dropwise addition of APS solution to the above solution, which was added over a period of half an hour. Lastly, the product was washed with deionized water and acetone and then dried under vacuum at 50 °C for 24 h.

FT-IR (KBr, ν cm^{-1})²⁶: 3400 (-NH-), 1713 (-C=O), 1560 (quinoid ring), 1480 (benzenoid ring), 802 (aromatic -CH)

¹HNMR (400 MHz, DMSO)²⁶: δ 9.46 ppm (protons of carboxylic acid), δ 6–8 ppm (protons of benzene rings in the benzenoid and quinoid forms), δ 4 ppm (N-H groups in the polymer backbone)

Synthesis of Fe₃O₄ magnetic nanoparticles

Fe₃O₄ nanoparticles were synthesized via co-precipitation method.²⁷ Briefly, FeCl₃·6H₂O, and FeCl₂·4H₂O (with the molar ratio of 2:1, respectively) were dissolved in 50 mL deionized water at room temperature, and was stirred mechanically at 80 °C for 15 min. 10 mL of NH₄OH (25%) was quickly added into the above mixture until the pH reached to 11. The resultant suspension was then refluxed at 80 °C for 2 h under vigorous stirring and N₂ atmosphere.

Finally, the black precipitate was separated by magnetic decantation, washed several times with deionized water and ethanol, dried at 50 °C in a vacuum oven for 6 h.

FT-IR (KBr, ν cm^{-1})²⁷: 3369 (-OH), 670 (Fe–O–Fe)

Synthesis of poly (aniline-co-3-aminobenzoic acid) @Fe₃O₄ core-shell nanocomposite

The poly (aniline-co-3-aminobenzoic acid) @ Fe₃O₄ (PA3ABA@Fe₃O₄) core-shell nanocomposite was synthesized via the in-situ copolymerization technique. First 0.5 g of Fe₃O₄ nanoparticles were dispersed in 50 ml of HCl solution (1 M) by sonication bath for 1 h. Afterwards, 1 g (0.010 mol) of Ani monomer and 1.46 g (0.010 mol) of 3ABA were added to above mixture and then mixture was dispersed under magnetic stirring for 30 min and ultrasonication for 40 min to obtain a uniform mixture. Then APS solution (1.25 g in 20 ml H₂O) was added to pervious mixture drop by drop for 30 min. The reaction was allowed to proceed for 24 h under magnetic stirring. Finally, obtained black precipitate washed with deionized water and acetone several times and dried in vacuum oven at 60 °C for 48 h.

Adsorption studies

The PA3ABA copolymer and PA3ABA@Fe₃O₄ nanocomposite were utilized as adsorbents for the removal of Pb(II) from aqueous solution. Adsorption experiments were carried out by the batch method.²⁸ The adsorption equilibrium experiments include the effect of pH values (4.0 – 8.0), amount of adsorbent (20-60 mg), initial concentration of Pb(II) (10–100 mgL⁻¹), and immersion time (10-90 min) on adsorption, determination of the maximum binding capacity, isotherm, and kinetic of adsorption. The effect of each factor was showed at constant conditions of 0.05 g adsorbent powder dispersed in 25 mL of Pb(II) solution (50 mg L⁻¹) for 90

min with stirring at 300 rpm and 298 K, varying the initial level of related factor. After the equilibrium in all experiments, the two phases were separated and the concentration of Pb(II) was analyzed by using AAS. The adsorption percentage of Pb(II) (S %) was calculated using following equation:¹⁸

$$S\% = \left(\frac{C_i - C_e}{C_i} \right) \times 100 \quad (1)$$

where C_i and C_e are the initial and final concentration of Pb(II) in solution (mg/L) before and after sorption, respectively.

Adsorbent regeneration and reuse

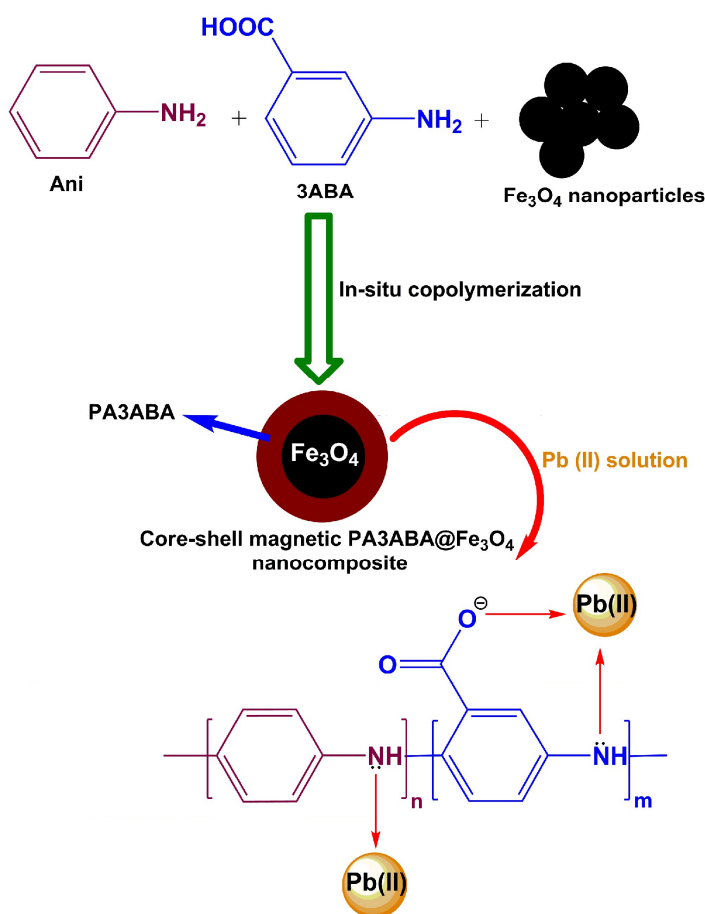
Three consecutive adsorption-desorption cycles were performed to test the reusability of PA3ABA and PA3ABA@Fe₃O₄ nanocomposite. Each adsorption process was carried out in batch experiment for 12 h. Then, the adsorbent was magnetically separated from the solution and then washed gently with distillation water to remove the adhered solution. The collected adsorbent was then dispersed into 50 mL of 0.1 M HCl and shaken at 180 rpm shortly for 10 min to regenerate the adsorbent. Prior to the next cycle, the regenerated adsorbent was washed repeatedly with distillation water until the effluent was neutral (pH 7). The desorption percentage (D %) was calculated as follows:¹⁷

$$\%D = \frac{A}{B} \times 100 \quad (2)$$

where A is the amount of Pb(II) desorbed to the elution medium (mg) and B is the amount of Pb(II) adsorbed on the adsorbent (mg)

Results and discussion

Water is the most vital compound on the earth for the human activities. Safe water supply is the main requirement of the human being for their better health. Water contamination by heavy metal ions is rising global due to quick growth of industry. Therefore, the removal of heavy metal ions from water is important concern in development countries. In the current study, we presented PA3ABA@Fe₃O₄ core-shell nanocomposite as a super adsorbent for Pb(II) removal from water. Scheme 1 shows the schematic illustration of the fabrication route to prepare PA3ABA@Fe₃O₄ core-shell nanocomposite and uptake mechanism of Pb(II) from water.



Scheme 1. Schematic pathway to prepare PA3ABA@Fe₃O₄ core-shell nanocomposite and uptake mechanism of Pb(II) from water.

Characterization of adsorbents

Fig. 1 shows the FT-IR spectra of PA3ABA, Fe_3O_4 and PA3ABA@ Fe_3O_4 magnetic nanocomposite. The peaks at 1550, and 1460 cm^{-1} for PA3ABA@ Fe_3O_4 nanocomposite were assigned to the stretching vibration for the quinoid, and benzenoid moieties of PA3ABA, respectively.²⁶ A medium peak at 1703 cm^{-1} was related to C=O stretching vibrations of the carboxylic groups in PA3ABA.²⁶ In addition, the absorption bands at around 550 cm^{-1} can be ascribed to the Fe–O–Fe stretching vibration of Fe_3O_4 .²⁹ The peaks shift observed in the FTIR spectrum of the PA3ABA@ Fe_3O_4 nanocomposite might be ascribed to the intermolecular interaction between hydroxyl groups of Fe_3O_4 and carboxylic groups of PA3ABA.

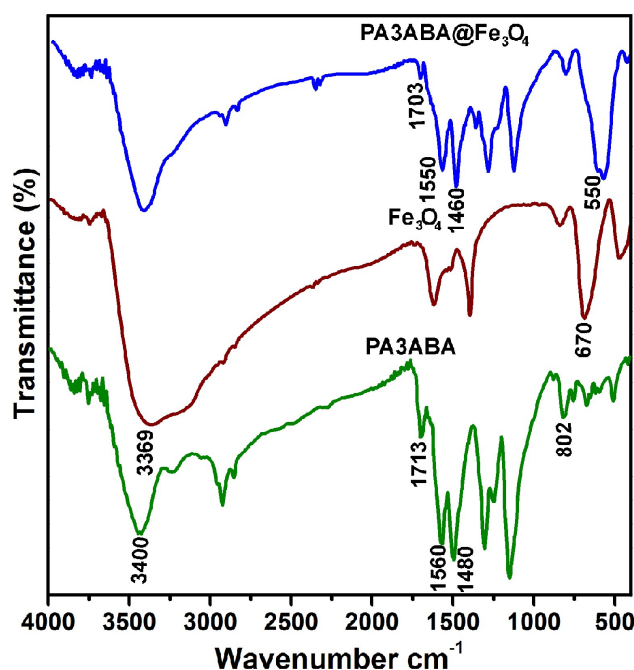


Fig. 1. FTIR spectra of PA3ABA, Fe_3O_4 , and PA3ABA@ Fe_3O_4 nanocomposite

The XRD pattern was used for the phase study on the crystallized product. Fig. 2 shows the XRD patterns of PA3ABA, Fe_3O_4 and PA3ABA@ Fe_3O_4 nanocomposite. The XRD pattern of Fe_3O_4 displayed a highly orderly stacked structure.³⁰ Bare PA3ABA copolymer showed a

typical semicrystalline pattern, whereas for the PA3ABA@Fe₃O₄ nanocomposite, the XRD pattern exhibited a nearly crystalline structure.²⁶ The characteristic peaks related to the Fe₃O₄ nanoparticles and PA3ABA copolymer were observed in the XRD pattern of PA3ABA@Fe₃O₄ nanocomposite. Therefore, according to the above discussion, it can be concluded that the PA3ABA@Fe₃O₄ nanocomposite was successfully synthesized.

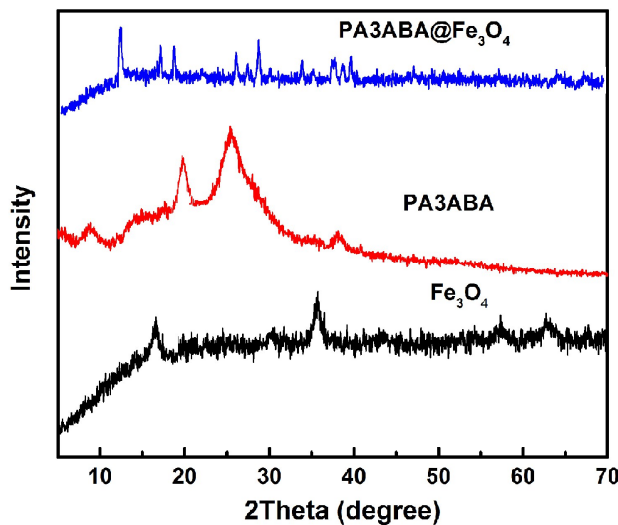


Fig. 2. XRD patterns of the PA3ABA, Fe₃O₄ nanoparticles and PA3ABA@Fe₃O₄ nanocomposite

The SEM (Fig. 3a and 3b) and TEM (Fig. 3c) micrographs were performed to determine the structure and morphology of the synthesized PA3ABA and PA3ABA@Fe₃O₄ nanocomposite. Accordingly, the PA3ABA (Fig. 3a) demonstrated a well-defined spherical shape with an average diameter of 90 nm. The SEM image of the PA3ABA@Fe₃O₄ nanocomposite (Fig. 3b) displayed sphere-like structures with the size distribution of around 100–200 nm in diameter. Fig. 3c shows TEM image of the PA3ABA@Fe₃O₄ core-shell nanocomposite. The TEM micrograph of the PA3ABA@Fe₃O₄ nanocomposite exhibited well-defined, core-shell structures with an average

particle size diameter of 50 nm. The Fe_3O_4 core, after it was coated with the PA3ABA shell, was much darker than the pre-coated magnetite nanoparticles.

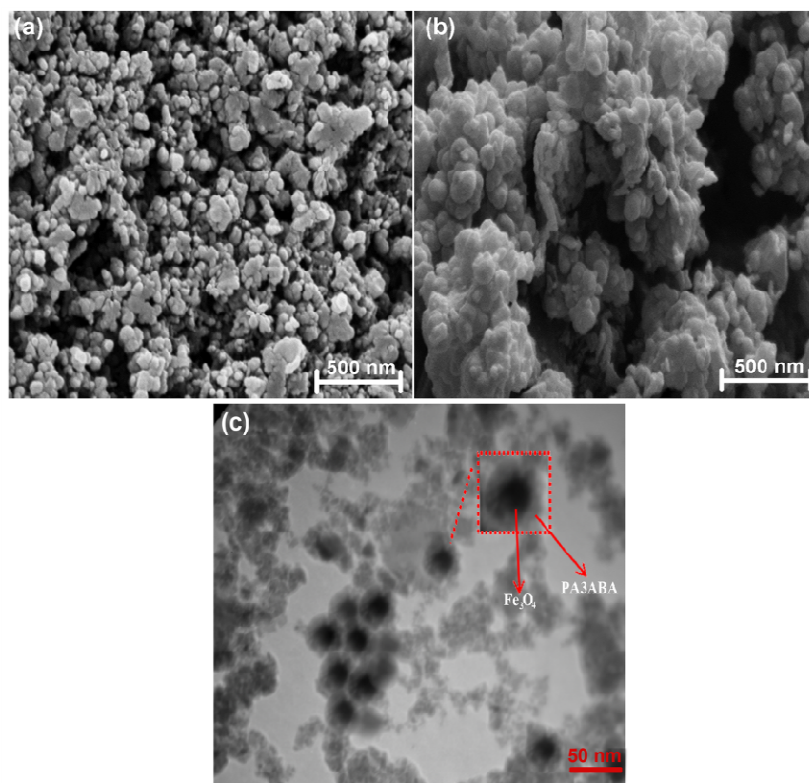


Fig. 3. The SEM micrographs of PA3ABA (a), and PA3ABA@ Fe_3O_4 nanocomposite (b) and TEM image of PA3ABA@ Fe_3O_4 nanocomposite (c)

Fig. 4 illustrates the magnetization hysteresis loops of the Fe_3O_4 nanoparticles and PA3ABA@ Fe_3O_4 nanocomposite at room temperature. Saturation magnetization (M_S) value of Fe_3O_4 nanoparticles was 50.5 emu g^{-1} . The adsorbed PA3ABA on the surface of Fe_3O_4 nanoparticles in the nanocomposite leads to a decrease in saturation magnetization value, 37.8 emu g^{-1} . The reduction in M_S value may be attributed to (I) the lower content of the magnetic component in the PA3ABA@ Fe_3O_4 nanocomposite; (II) the part magnetization of magnetic Fe_3O_4 nanoparticles is shielded by the electro-conductive PA3ABA copolymer. To the best of

our knowledge, small coercivity (H_c) and remanence (M_r) in the absence of the external magnetic field indicated the super-paramagnetic property of materials.²⁹ Therefore, according to the obtained results, it was concluded that both Fe_3O_4 nanoparticles and $PA3ABA@Fe_3O_4$ nanocomposite were super-paramagnetic.

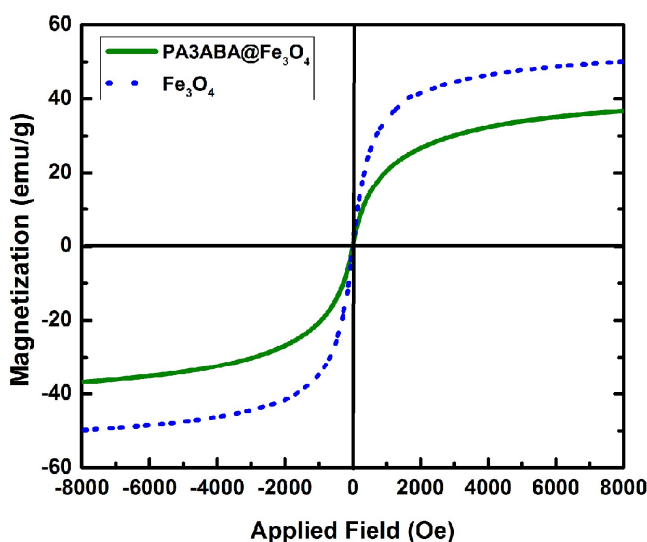


Fig. 4. VSM of Fe_3O_4 nanoparticles, and $PA3ABA@Fe_3O_4$ nanocomposite

Thermogravimetric analysis (TGA) was used to evaluate the thermal stability of synthesized materials. Fig. 5 demonstrates the TGA thermograms of Fe_3O_4 , PA3ABA, and $PA3ABA@Fe_3O_4$ nanocomposite under nitrogen atmosphere. TGA thermogram of Fe_3O_4 nanoparticles showed two-step decomposition. The first step was observed at 80 – 120 °C (around 2% weight loss) and the second step at 120-300 °C (around 3% weight loss), which were related to removal of water during dehydration of surface hydroxyl groups and thermal crystal phase transformation of Fe_3O_4 to Fe_2O_3 , respectively.^{9,2,4} On the other hand, in the TGA thermogram of PA3ABA the weight loss about 8% (45 to 150°C) related to the loss of moisture, volatilization of the solvent, and adsorbed HCl.³¹ The weight loss about 10% (150 to 450°C) is due to the loss of low molecular weights, and CO_2 . The third weight loss (9.5%) occurring

between 400 and 600°C associated to the final degradation of the copolymer. As seen from the TGA thermogram of the PA3ABA@Fe₃O₄ nanocomposite, the residual weight of nanocomposite at 700 °C was about 78.5 wt%, which was higher than that of the PA3ABA copolymer. Therefore, the presence of the Fe₃O₄ nanoparticles can result in the improvement of the thermal stability of the PA3ABA@Fe₃O₄ nanocomposite by acting as the thermal barrier to protect the PA3ABA from the thermal degradation.

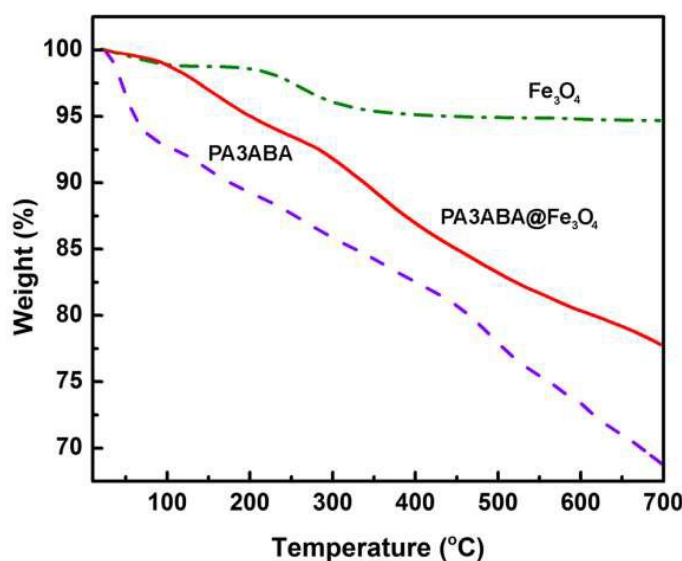


Fig. 5. TGA thermograms of Fe₃O₄ nanoparticles, PA3ABA, and PA3ABA@Fe₃O₄ nanocomposite

Adsorption studies

Effect of solution pH on Pb(II) adsorption

The initial pH of solution is a significant factor affecting the adsorption of heavy metal ions. To avoid chemical precipitation, adsorption experiments were done at three different initial pH levels viz., 4, 6 and 8. Fig. 6a illustrates the effect of pH on the adsorption of Pb(II). When pH was 4, the adsorption percentage for Pb(II) was low. The competitive adsorption between Pb(II)

and available proton for protonation of the adsorbent is a reasonable response for this phenomenon. The removal percentage of Pb(II) increased gradually with increasing solution pH from 4.0 to 6.0 and slightly diminished at 8.0. With the increase of solution pH, the concentration of H^+ decreases and more surface functional groups are deprotonated to provide available sorption sites for Pb(II), leading to the increase of sorption percentage. As shown in Fig. 6a, the maximum removal percentage (% S) of Pb(II) for both PA3ABA copolymer and PA3ABA@Fe₃O₄ nanocomposite were 82% and 89% at pH 6.0, respectively. Mainly, the presence of amine and carboxyl groups on the copolymer backbone together with Fe₃O₄ nanoparticles may result in the formation of Pb(II) complexes through chelating or metal exchanges in the adsorbents.

Effect of adsorbent dosage on sorption of Pb(II)

The amount of adsorbents is very important parameter as it determines the extent of removal of metal ion and maybe used to define the cost of adsorbent per unit volume of solution to be treated.¹³ The removal percentage of Pb(II) as a function of the adsorbent dosage was investigated at room temperature for 90 min and at pH 6.0 by varying the amount of the adsorbent from 20 to 60 mg in 50 mL of Pb(II) solution (50 mg L⁻¹) and the results are revealed in Fig. 6b. As can be seen in Fig. 6b, the adsorption of the Pb(II) increased with increasing the amount of adsorbents. This increase in the adsorption could be due to presence of more binding sites on the surface of adsorbents to form complexes with Pb(II). However, the optimum amount of PA3ABA copolymer and PA3ABA@Fe₃O₄ nanocomposite for further adsorption experiments was selected as 50 mg, due to the maximum adsorption happened for 50 mg of adsorbents and further increase in adsorbent dosage had less influence on removal of Pb(II). This can probably suggest that adsorption of Pb(II) occurs mostly with active sites on the surface of samples. As

seen in Fig. 6b, it is clear that the adsorption performance of Pb(II) by PA3ABA@Fe₃O₄ nanocomposite was better than PA3ABA copolymer.

Effect of contact time on Pb(II) adsorption

The contact time is a main parameter for an effective use of adsorbent for practical applications and finding the optimum time for complete removal of the particular metal ions.³² Fig. 6c shows the influence of contact time on the adsorption of the Pb(II) in the range 10-90 min for 50 mg of PA3ABA copolymer and PA3ABA@Fe₃O₄ nanocomposite at a constant stirring rate. As shown in Fig. 6c, an increase in adsorption efficiency as the contact time increases up to 50 min and remains almost constant after that. The removal percentage of Pb(II) for the PA3ABA copolymer and PA3ABA@Fe₃O₄ nanocomposite at initial concentration of Pb(II) (50 mgL⁻¹) was calculated 82.5% and 88.5%, respectively. The removal percentage of Pb(II) in PA3ABA@Fe₃O₄ nanocomposite was higher than that of PA3ABA copolymer which can be ascribed to the large surface area of PA3ABA@Fe₃O₄ nanocomposite as well as homogenous of nanoparticles in the nanocomposite leading to a high content of active chelating sites.

Effect of initial Pb(II) concentration on adsorption

It's known; the rate of adsorption is an imperative factor for effective adsorption and depends on the initial concentration of metal ion.³³ The removal percentage of Pb(II) at different concentrations (10–100 mg L⁻¹), keeping all other factors constant and using PA3ABA copolymer and PA3ABA@Fe₃O₄ nanocomposite adsorbents, is revealed in Fig. 6d. When the initial concentration of Pb(II) increased, the removal percentage decreased slightly from 90% and 88% for PA3ABA copolymer and PA3ABA@Fe₃O₄ nanocomposite to 65% and 70%, respectively. The decrease in adsorption could be due to the fact that at higher initial

concentration the active surface sites of PA3ABA copolymer and PA3ABA@Fe₃O₄ nanocomposite adsorbents were saturated.

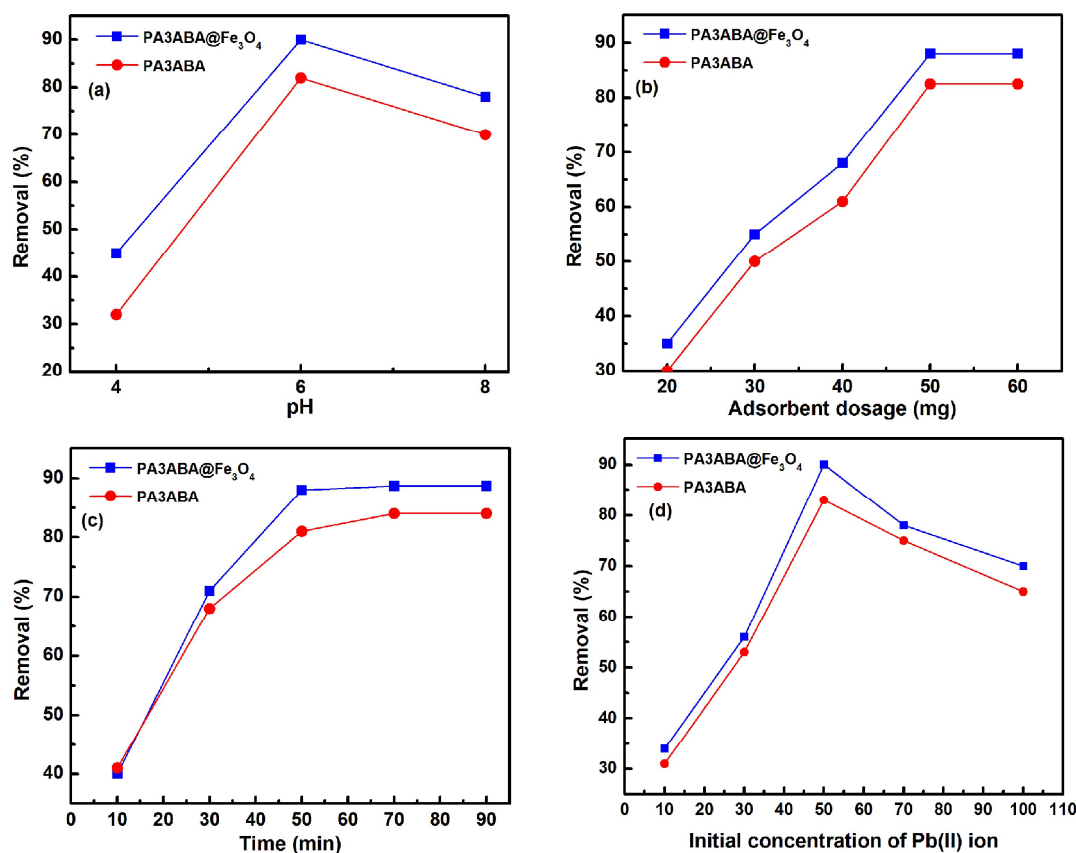


Fig.6. Effect of pH (a), adsorbent dosage (b), contact time (c), and initial concentration of Pb(II) (d) on the Pb(II) adsorption

FTIR of PA3ABA@Fe₃O₄ – Pb(II) complex

To the best of our knowledge, the metal complexation to a certain polymeric ligand causes changes in the absorption spectrum of the starting polymer. The FT-IR spectroscopy was used for the characterization of PA3ABA@Fe₃O₄ nanocomposite–Pb(II) complexes because of the frequency at which a characteristic group of the adsorbent polymer was modified by metal ion complexation, the shift or absence of a certain band presence in the starting ligand as well as

the presence of new bands being observed. The FTIR spectra of PA3ABA@Fe₃O₄ nanocomposite (before and after sorption) are shown in Fig. 7. The comparison of these IR spectra showed that some characteristic peaks and reduction in peak intensity together with shift of vibration bands indicated that bonding between the ligand and Pb(II) was covalent or ionic in nature. These evidences confirmed complexation between Pb(II) and amine and carboxylic groups in the structure of nanocomposite.

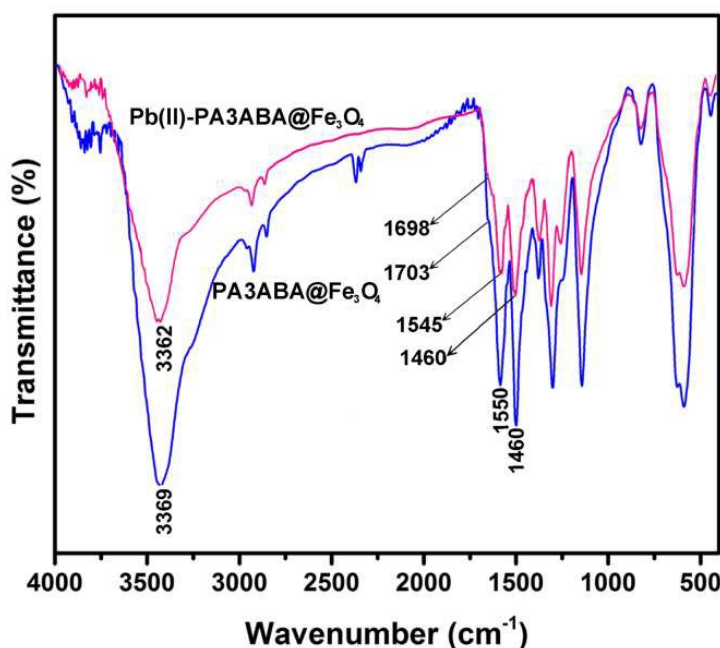


Fig.7. FTIR of PA3ABA@Fe₃O₄ nanocomposite before and after sorption of Pb(II)

Desorption and reuse study

To evaluate the possibility of regeneration and recycle of the PA3ABA and PA3ABA@Fe₃O₄ nanocomposite adsorbents, adsorption–desorption experiments were done. Since the metal complexes are dissociated in acidic medium batch, desorption studies were shown in the acidic conditions (HCl, 0.1 M) and desorption efficiencies were subsequently compared. Fig. 8 displays the association between the number of reuse cycles and the adsorption percentage of the

regenerated adsorbents. The results displayed that the desorption percentage of the Pb(II) decreased to about 75% and 80% for PA3ABA copolymer and PA3ABA@Fe₃O₄ nanocomposite, respectively, after three cycles. It can be concluded that the PA3ABA copolymer and PA3ABA@Fe₃O₄ nanocomposite beads can be used repeatedly with negligible loss of adsorption capacity for the representative Pb(II).

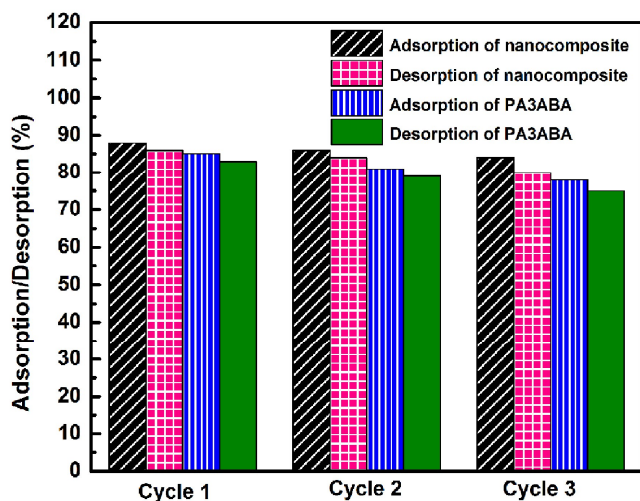


Fig. 8. Adsorption/desorption percentages of Pb(II) during 3 cycles

Isotherm Studies

The adsorption isotherms of Pb(II) on PA3ABA copolymer and PA3ABA@Fe₃O₄ nanocomposite are exposed in Fig. 9. In order to know the adsorption mechanism better, the experimental data were adopted by Langmuir, and Freundlich isotherm models. Langmuir model accepts that the bulk phases and surfaces of homogeneous sorbents show an ideal behavior with all the adsorption sites identically and energy equivalently.³⁴ It has been widely used to describe the monolayer and short-term sorption processes. On the other hand, Freundlich model is based on the sorption on reversible heterogeneous surfaces.⁹ The Langmuir (Eq. 3), and Freundlich (Eq. 4) adsorption isotherm models are presented as follows:¹⁸

$$\frac{C_e}{Q_e} = \frac{1}{Q_m K_L} + \frac{C_e}{Q_m} \quad (3)$$

$$\text{Log } Q_e = \text{Log } K_F + \frac{1}{n} \text{Log } C_e \quad (4)$$

where Q_e (mg/g) is the equilibrium adsorption capacity of Pb(II) on the adsorbent; C_e (mg/L), is Pb(II) concentration at equilibrium; Q_{\max} (mg/g) is the maximum uptake capacity of adsorbent; K_L (Lmg⁻¹) and K_F (Lmg⁻¹) are the Langmuir, and Freundlich adsorption constants, respectively; $1/n$ is intensity of the adsorption. The Langmuir, and Freundlich isotherm plots for Pb(II) and the adsorption isotherm parameters are shown in Fig.9 and summarized in Table 1, respectively. By comparing the correlation coefficient (R^2) values of Langmuir, and Freundlich isotherms for the Pb(II), we can find the most respective and suitable model for fitting the experimental data. According to the obtained results (Table 1), the corresponding correlation coefficient (R^2) for the PA3ABA copolymer was as high as 0.99 representative that the electro sorption of Pb(II) fits well with the Langmuir isotherm. On the other hand, after comparing the corresponding correlation coefficient (R^2) of two isotherm models, it can easily be found that the Freundlich isotherm was best fitted to the experiment results over the Langmuir isotherm, demonstrating that the adsorption of Pb(II) on PA3ABA@Fe₃O₄ nanocomposite is of a monolayer type where interactions between adsorbed molecules are small.

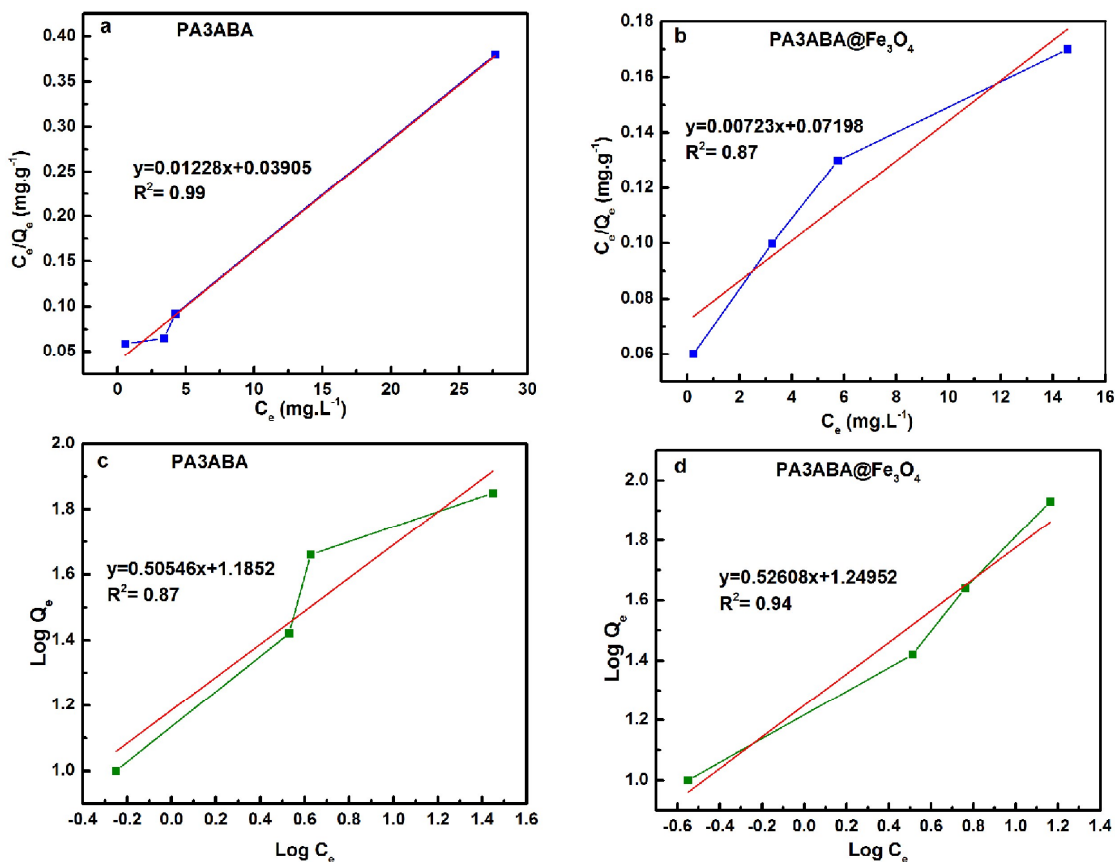


Fig. 9. Langmuir (a and b) and Freundlich (c and d) adsorption isotherm models of PA3ABA copolymer and PA3ABA@Fe₃O₄ nanocomposite for Pb(II) (Temperature, 25°C; contact time, 70 min; C₀ = 10–70 mg L⁻¹; adsorbent dosage, 50 mg; pH 6)

Table 1. Isotherm model parameters and correlation coefficients for Pb(II)

Adsorbent	Langmuir model			Freundlich model		
	Q _m (mgg ⁻¹)	K _L (Lmg ⁻¹)	R ²	K _F (Lmg ⁻¹)	n	R ²
PA3ABA	81.43	0.31	0.99	15.31	1.97	0.87
PA3ABA@Fe ₃ O ₄	138.31	0.10	0.87	17.76	1.90	0.94

Kinetic studies

Adsorption kinetics were studied to estimate both the rate of Pb(II) sorption and the equilibrium time required for the adsorption isotherm. The experiments were examined in the range of 10-90 min at room temperature using 50 mg of adsorbents for 50 mL of Pb(II) solution (50 mg/L). Adsorption rates were studied using two kinetic models, i.e., the pseudo-first-order and the pseudo-second-order models. The Lagergren pseudo-first-order kinetic and pseudo-second-order models are based on the adsorption rate relates to the number of the unoccupied adsorptive sites, and predict the kinetic behavior of adsorption with chemical sorption being the rate-controlling step, respectively.^{11,21} The Lagergren pseudo-first-order model (Eq. 5), and pseudo-second-order model (Eq. 6) are presented as follows:¹⁸

$$\text{Log}(Q_e + Q_t) = \text{Log} Q_e - \frac{k_1}{2.303} t \quad (5)$$

$$\frac{t}{Q_t} = \frac{1}{k_2 Q_e^2} + \frac{1}{Q_e} t \quad (6)$$

Where Q_t is the adsorption capacity of Pb(II) on an adsorbent at time t ($\text{mg}\cdot\text{g}^{-1}$); k_1 (min^{-1}) and k_2 ($\text{g}\ \text{mg}^{-1}\text{min}^{-1}$) are the rate constants of the pseudo-first order and pseudo-second-order, respectively. Kinetic plots and parameters of two models were calculated and are given in Fig 10 (a and b) and Table 2.

As seen in Fig. 10, the pseudo-first-order model was to predict the behavior of the adsorption process of synthesized adsorbents. Furthermore, the correlation coefficients R^2 for the pseudo-first-order kinetic model obtained for the PA3ABA copolymer and PA3ABA@Fe₃O₄ nanocomposite were higher than the R^2 for pseudo-second-order kinetic model (Table 2). Moreover, the $Q_{e,\text{cal}}$ values as obtained from the pseudo-first-order kinetic model appeared to be very close to the experimentally observed values than the values from the pseudo-second-order

kinetic model (Table 2). Therefore, suggesting that the adsorption process maybe controlled by physical adsorption which might include the complexation reaction between Pb(II) and adsorbents.

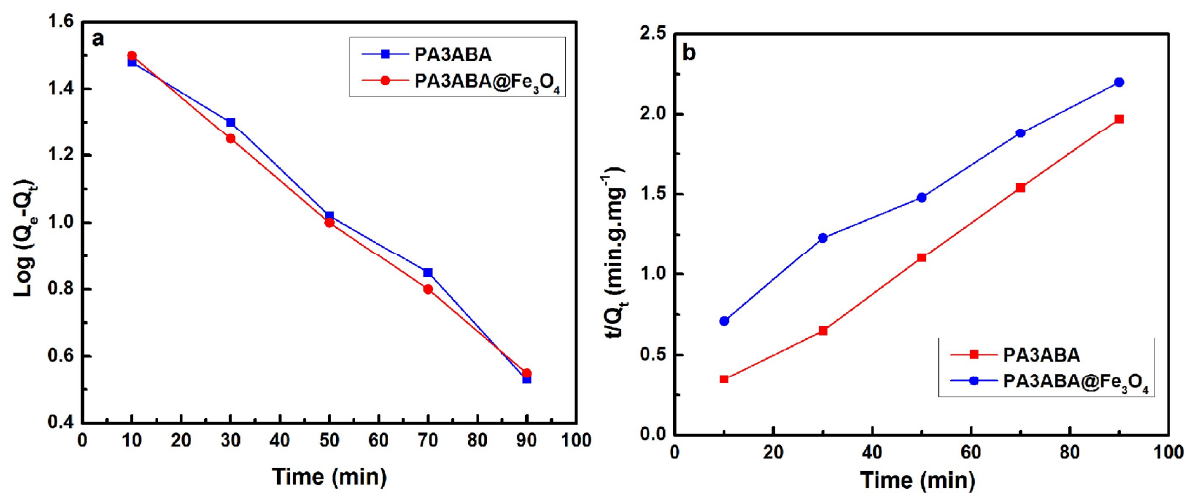


Fig. 10. Kinetic models for the adsorption of Pb(II): pseudo-first-order (a), pseudo-second-order (b). (Temperature, 25°C; C₀ =50 mgL⁻¹; adsorbent dosage, 50 mg; pH 6)

Table 2. Kinetic models and their statistical parameters at 25°C and pH 6.0 for Pb(II)

Adsorbent	Pseudo first order				Pseudo second order		
	Q _{e,exp} (mg g ⁻¹)	k ₁ (min ⁻¹)	Q _{e,cal} (mg g ⁻¹)	R ²	k ₂ (min ⁻¹)	Q _{e,cal} (mg g ⁻¹)	R ²
PA3ABA	41.54	0.027	42.02	0.99	0.0005	54.94	0.98
PA3ABA@Fe ₃ O ₄	40.35	0.031	41.68	0.97	0.0047	48.30	0.99

Comparison with other adsorbents

For further comparison with other various adsorbents, the adsorption capacity (Q_m) of different adsorbents reported in the literature is listed in Table 3. According to this table, the adsorption capacity of PA3ABA copolymer and PA3ABA@Fe₃O₄ nanocomposite was much higher than the reported adsorbents, indicating that PA3ABA copolymer and PA3ABA@Fe₃O₄ nanocomposite were more promising candidates for effective adsorption of Pb(II) from aqueous solution.

Table 3. Comparison of adsorption capacity of various adsorbents for Pb(II) adsorption

Adsorbent	Q(mg/g)	Reference
PA3ABA	81.43	Present Research
PA3ABA@Fe ₃ O ₄ nanocomposite	138.31	Present Research
Magnetic chitosan grafted thiacalix[4]arene	23.25	18
Graphitic carbon nitride	65.60	34
Montmorillonite–kaolinite/TiO ₂ nanocomposite	71.10	35
Polythiophene/Sb ₂ O ₃ nanocomposite	18.94	7
Rice Straw/Fe ₃ O ₄ nanocomposite	19.45	36
Poly(acrylic acid)/bentonite nanocomposite	93.01	37
Bentonite	52.31	37

Conclusions

In summary, the poly (aniline-co-3-aminobenzoic acid)@Fe₃O₄ core-shell nanocomposite was fabricated by using a two-step method. The poly (aniline-co-3-aminobenzoic acid)@Fe₃O₄ core-shell nanocomposite could remove Pb(II) from aqueous solution with adsorption capacity, 138.31 mg/g at room temperature. Experimental studies of Pb(II) removal displayed that the poly (aniline-co-3-aminobenzoic acid)@Fe₃O₄ core-shell nanocomposite had considerably higher adsorption capacities for Pb(II) than that of the poly (aniline-co-3-aminobenzoic acid)

copolymer. Langmuir and Freundlich models were most suitable to fit the adsorption data of poly (aniline-co-3-aminobenzoic acid) copolymer and poly (aniline-co-3-aminobenzoic acid)@Fe₃O₄ core-shell nanocomposite, where the poly (aniline-co-3-aminobenzoic acid)@Fe₃O₄ core-shell nanocomposite exhibited higher maximum adsorption capacity than the poly (aniline-co-3-aminobenzoic acid) copolymer. The adsorption kinetics of poly (aniline-co-3-aminobenzoic acid) and poly (aniline-co-3-aminobenzoic acid)@Fe₃O₄ core-shell nanocomposite were well described by pseudo-first-order model. The poly (aniline-co-3-aminobenzoic acid)@Fe₃O₄ core-shell nanocomposite could be an appropriate candidate for water treatment process.

References

1. X. Du, H. Zhang, X. Hao, G. Guan, and A. Abudula, *ACS Appl. Mater. Interfaces*, 2014, **6**, 9543–9549.
2. F. Fu and Q. Wang, *J. Environ. Manage.*, 2011, **92**, 407–18.
3. S. Li, Y. Wei, Y. Kong, Y. Tao, C. Yao, and R. Zhou, *Synth. Met.*, 2015, **199**, 45–50.
4. H. Wang, X. Yuan, Y. Wu, X. Chen, L. Leng, H. Wang, H. Li, and G. Zeng, *Chem. Eng. J.*, 2015, **262**, 597–606.
5. E. N. Zare, M. M. Lakouraj, and M. Mohseni, *Synth. Met.*, 2014, **187**, 9–16.
6. P. N. Moghadam and E. N. Zareh, *e-Polymers*, 2010, 1–9.
7. R. Khalili, F. Shabanpour, and H. Eisazadeh, *Adv. Polym. Technol.*, 2014, **33**, 21389(1 of 7).
8. E. N. Zare and M. M. Lakouraj, *Iran. Polym. J.*, 2014, 1–10.
9. E. N. Zare, M. M. Lakouraj, and A. Ramezani, *Adv. Polym. Technol.*, 2015, **34**, 21501 (1–11).
10. A. Eisazadeh, H. Eisazadeh, and K. A. Kassim, *Synth. Met.*, 2013, **171**, 56–61.
11. Y. Kong, J. Wei, Z. Wang, T. Sun, C. Yao, and Z. Chen, *J. Appl. Polym. Sci.*, 2011, **122**, 2054–2059.
12. C. Eng and R. Samani, *Iran. J. Chem. Chem. Eng*, 2011, **30**, 97–100.
13. T. Hasani and H. Eisazadeh, *Synth. Met.*, 2013, **175**, 15–20.
14. M. Ghorbani and H. Eisazadeh, *Synth. Met.*, 2012, **162**, 1429–1433.
15. M. Choi and J. Jang, *J. Colloid Interface Sci.*, 2008, **325**, 287–9.
16. E. N. Zare, M. M. Lakouraj, P. N. Moghadam, and R. Azimi, *Polym. Compos.*, 2013, **34**, 732–739.
17. M. M. Lakouraj, F. Mojerlou, and E. N. Zare, *Carbohydr. Polym.*, 2014, **106**, 34–41.

18. M. M. Lakouraj, F. Hasanzadeh, and E. N. Zare, *Iran. Polym. J.*, 2014, **23**, 933–945.
19. J. Huang, R. Zhao, and H. Wang, *Water Res.*, 2010, **69**, 817–821.
20. X. Sun, L. Yang, Q. Li, Z. Liu, T. Dong, and H. Liu, *Chem. Eng. J.*, 2015, **262**, 101–108.
21. G. Zeng, Y. Liu, L. Tang, G. Yang, Y. Pang, Y. Zhang, Y. Zhou, Z. Li, M. Li, M. Lai, X. He, and Y. He, *Chem. Eng. J.*, 2015, **259**, 153–160.
22. Y. X. Zhang, X. Y. Yu, Z. Jin, Y. Jia, W. H. Xu, T. Luo, B. J. Zhu, J. H. Liu and X. J. Huang. *J. Mater. Chem.*, 2011, **21**, 16550-16557
23. Y. X. Zhang, Y. Jia, Z. Jin, X. Y. Yu, W. H. Xu, T. Luo, B. J. Zhu, J. H. Liu and X. J. Huang. *Cryst. Eng. Comm*, 2012, **14**, 3005-3007
24. Y. X. Zhang, Z. L. Liu, B. Sun, W. H. Xu and J. H. Liu. *RSC Adv.*, 2013, **3**, 23197-23206
25. Y. X. Zhang, Y. Jia. *Appl. Surf. Sci.*, 2014, **290**, 102-106
26. E. N. Zareh and P. N. Moghadam, *J. Appl. Polym. Sci.*, 2011, **122**, 97–104.
27. E. N. Zare, M. M. Lakouraj, and M. Baghayeri, *Int. J. Polym. Mater. Polym. Biomater.*, 2015, **64**, 175–183.
28. E. Erdem, N. Karapinar, and R. Donat, *J. Colloid Interface Sci.*, 2004, **280**, 309–14.
29. E. N. Zare, M. M. Lakouraj, M. Mohseni, and A. Motahari, *Carbohydr. Polym.*, 2015, **130**, 372–380.
30. M. M. Lakouraj, E. N. Zare, and P. N. Moghadam, *Adv. Polym. Technol.*, 2014, **33**, 21385(1–7).
31. M. S. Lashkenari and H. Eisazadeh, *Adv. Polym. Technol.*, 2014, **33**, 21466 (1–8).
32. A. G. Yavuz, E. Dincturk-Atalay, A. Uygun, F. Gode, and E. Aslan, *Desalination*, 2011, **279**, 325–331.
33. R. Norouzian and M. M. Lakouraj, *Synth. Met.*, 2015, **203**, 135–148.

34. R. Hu, X. Wang, S. Dai, D. Shao, T. Hayat, and A. Alsaedi, *Chem. Eng. J.*, 2015, **260**, 469–477.
35. A. B. Đukic, K. R. Kumric, N. S. Vukelic, M. S. Dimitrijevic, Z. D. Baščarevic, S. V. Kurko, L. L. Matović, *Appl. Clay. Sci.*, 2015, **103**, 20–27.
36. R. Khandanlou, M. B. Ahmad, H. R. Fard Masoumi, K. Shameli, M. Basri, and K. Kalantari, *Plos One*, 2015, 1-19.
37. H. R. Rafiei, M. Shirvani, O. A. Ogunseitan, *Appl. Water. Sci.*, 2014 (In press).

Efficient sorption of Pb(II) from aqueous solution using poly (aniline-co-3-aminobenzoic acid) - based magnetic core-shell nanocomposite

Ehsan Nazarzadeh Zare*, Moslem Mansour Lakouraj, Atefeh Ramezani

Polymer research laboratory, Department of Organic-Polymer Chemistry, Faculty of Chemistry, University of Mazandaran, Babolsar, Iran

*Corresponding author Email: ehsan.nazarzadehzare@gmail.com; Tel-fax: +981125342350; Postal code: 47416-95447

It can be proposed that PA3ABA@Fe₃O₄ core-shell magnetic nanocomposite is an appropriate candidate for water treatment process.

